Electrodeposition of ultrathin magnetic films of Fe and Co

W. Schindler,[a] O. Schneider, and J. Kirschner
Max–Planck–Institut für Mikrostrukturphysik, Weinberg 2, 06120 Halle, Germany

We electrodeposited ultrathin magnetic Fe and Co films on Cu(001) crystals from an aqueous 0.3 M Na_2SO_4/(Fe or Co)SO_4 electrolyte in a newly developed electrochemical cell. A deposition procedure of Fe from an organic electrolyte of propylene carbonate has been additionally developed to prevent the significant H_2 evolution during the Fe deposition from an aqueous electrolyte. Fe films of more than 8 monolayer (ML) thickness show the easy magnetization axis in plane. The saturation magnetization correlates linearly with the film thickness. In the thickness range between 2 and 8 ML, the easy magnetization axis is in the [001] direction. No magnetization is observed in films with thickness of less than 2 ML. Co films show in-plane magnetization with square hysteresis loops and a linear correlation of the saturation magnetization and film thickness above 2 ML. The magnetization vanishes at coverages of less than 1.5 ML as known from molecular beam epitaxy grown films. The coercive field of the Co films varies approximately linearly from 0.9 mT at 2.5 ML to 25 mT at 51 ML film thickness. © *1997 American Institute of Physics.* [S0021-8979(97)45508-1]

I. MOTIVATION

Electrochemically deposited films and particularly multilayers have attracted technological interest recently due to their exciting giant magnetoresistance (GMR).[1–3] Co based multilayers (CoPd, CoPt, CoCr), usually prepared by sputter or evaporation techniques, are discussed as materials for high density magneto-optical storage and perpendicular recording.[4–7] The electrochemical deposition of these films seems to be technologically interesting since the electrodeposition is a fast and cost effective deposition process useful to cover large areas and applicable to mass production.

The properties of electrodeposited single magnetic layers have so far been studied only on a few systems and in thickness ranges above μm, where the films grow polycrystalline.[8–12] Their characterization has usually been done *ex situ*. The magnetic properties, in particular, of electrodeposited ultrathin films in the monolayer (ML) range are so far not well investigated.

II. AQUEOUS ELECTROLYTE SOLUTIONS

We deposited ultrathin Fe and Co films in the ML range onto Cu(001) substrates under cleanliness conditions equivalent to UHV conditions of 5×10^{-10} mbar during molecular beam growth of films.[13] The electrochemical cell for the film deposition and *in situ* measurements of the magnetization by magneto-optical Kerr effect (MOKE) has been described in detail in Ref. 14.

The Cu(001) surface has been prepared by electropolishing in 65% H_3PO_4 for several minutes at $+1.8$ V against a carbon electrode. The crystal was then transferred into the cell under the protection of ultrapure water (Milli-Q plus) to prevent any degradation due to contact to the air.

The aqueous electrolyte consisted of 0.3 M Na_2SO_4/1 mM $CoSO_4$ for the Co deposition or 0.3 M Na_2SO_4/10 mM $FeSO_4$ for the Fe deposition. Oxygen has been removed from the electrolyte by degassing with ultrapure N_2 gas. A Pt wire was used as counter electrode, the potential of the Cu electrode has been measured against a standard calomel reference electrode. The deposition rate of the films was approximately 0.5 ML/s. This high deposition rate compared to that of a UHV deposition should be favorable for film stability in view of a possible room temperature instability of ultrathin magnetic films on Cu.[15]

The current–voltage characteristics of the Fe deposition is shown in Fig. 1. The current–voltage characteristics of the Co deposition is similar when taking the different standard potentials of Fe and Co into account. The films can be repeatedly deposited and dissolved by cycling the potential of the substrate. However, in the case of Fe, we find possibly an incomplete dissolution of the first monolayer Fe, observed as enhanced anodic current at potentials higher than the dissolution peak, between -400 and -100 mV. Therefore, in the case of Fe, the data have been determined from films which had been deposited onto a clean Cu surface.

The total anodic charge measured during the dissolution of Fe (dashed peak area in Fig. 1) is approximately 30% of the cathodic charge measured during the previous deposition of the film. The discrepancy results mainly from the simultaneous H_2 evolution at the Cu crystal at potentials lower than -900 mV. Therefore, we developed a deposition procedure for Fe from organic electrolytes, which does not show a simultaneous H_2 evolution (see Sec. III).

Fe films in the thickness range of 2 to $\approx$8 ML show the easy magnetization axis normal to the surface (Fig. 2, open circles). The easy magnetization direction of films thicker than 8 ML is in plane (Fig. 2, full circles). This magnetic behavior is similar to that observed in molecular beam epitaxy (MBE) grown Fe/Cu(001) films, from which is known that evaporated Fe on Cu(001) at room temperature shows a fcc/bcc phase transition at a thickness of approximately 10 ML.[16]

Co films show square hysteresis loops (inset of Fig. 3) indicating a uniform thickness across the measured surface area of 1 mm^2. The easy magnetization axis is in plane as is

[a]Electronic mail: schi@mpi-msp-halle.mpg.de

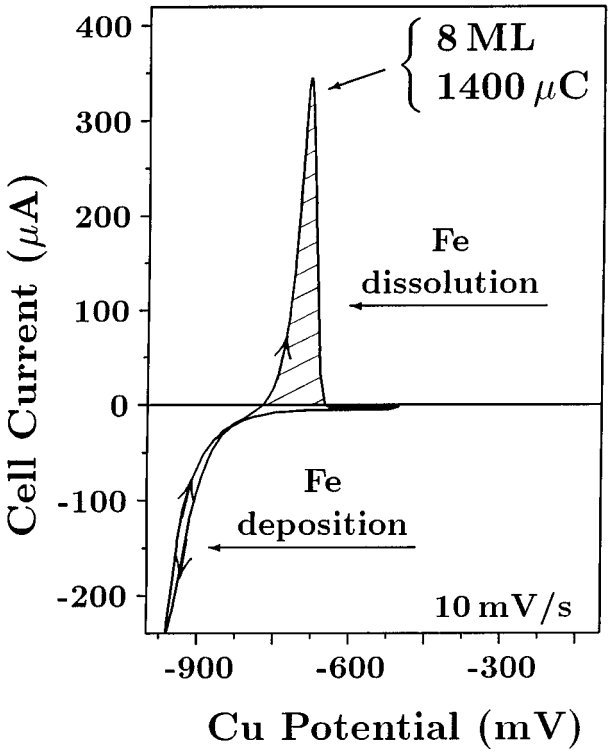

FIG. 1. Current–voltage characteristics of the Fe deposition from an aqueous electrolyte of 0.3 M Na_2SO_4 and 10 mM $FeSO_4$. The arrows indicate the cycling direction (with 10 mV/s) of the deposition/dissolution of the Fe films. The deposition has been done at potentials below −900 mV. The anodic peak around −700 mV (dashed area) represents the dissolution of the previously deposited Fe film. The peak area is equivalent to a charge of 1400 μC or a film thickness of 8 ML. The MOKE measurements are done at around −780 mV where no external current flows to or from the substrate.

known from MBE grown Co films. The saturation magnetization above 2 ML depends linearly on the film thickness as shown in Fig. 3. The magnetization vanishes below a coverage of ≈1.5 ML due to the decreasing Curie temperature and

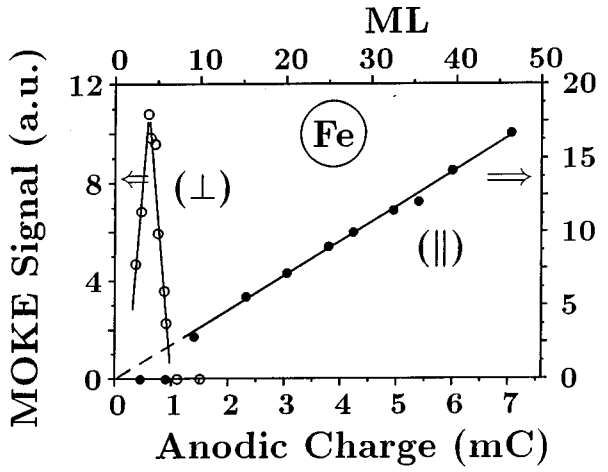

FIG. 2. Dependence of the total saturation magnetization of Fe films on the number of ML (upper x scaling) corresponding to the deposited charge (lower x scaling). Open circles (left y scaling): easy magnetization axis out-of-plane (⊥); full circles (right y scaling): easy magnetization axis in plane (∥; magnetic field applied in [110] direction). The linear fit through the data points of the in-plane saturation magnetization extrapolates to zero for 0 ML film thickness.

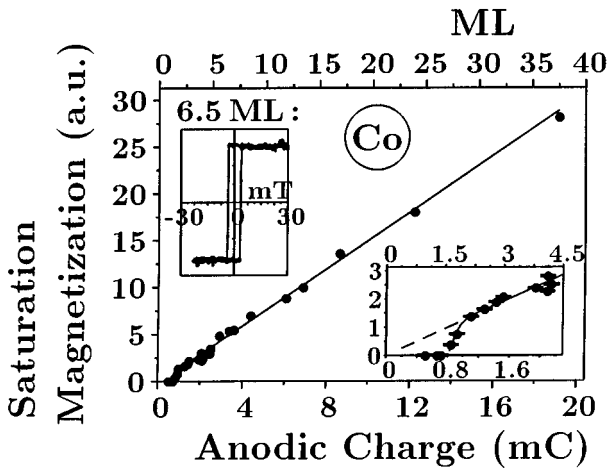

FIG. 3. Dependence of the total saturation magnetization of Co films on the number of ML (upper x scaling). The lower x scaling is the equivalent deposited charge. The magnetic field was applied in the easy [110] direction. The left-hand side inset shows the hysteresis loop for 6.5 ML. The right-hand side inset shows the range from 0 to 4.5 ML thickness. The error bars indicate ±0.2 ML. The linear fit through the data above 2 ML thickness extrapolates to zero for 0 ML film thickness, demonstrating the absence of magnetically dead layers.

the lack of film percolation. This behavior is compatible with the partial bilayer growth mode in evaporated Co/Cu(001).[17]

The coercive fields of our Co films are approximately ten times larger than those observed in MBE grown films of comparable thickness. They vary approximately linearly from 0.9 mT at 2.6 ML to 25 mT at 51 ML film thickness. Possible reasons for this large coercivity may be the deposition near the thermodynamical equilibrium resulting in a different growth behavior than that known from MBE films and our substrate surface quality, which is still rough (up to 10 nm height variation on 1 μm length scale) compared to UHV prepared Cu(001) crystals.

The linear correlation of saturation magnetization and film thickness extrapolates to zero for 0 ML thickness both for Fe and Co (Figs. 2 and 3), clearly showing that there are no ''magnetically dead'' layers in our electrodeposited films.

III. NONAQUEOUS ELECTROLYTE SOLUTIONS

The electrochemical cell and experimental procedure have been similar to that described above.

Propylene carbonate (PC) has been dried over activated mole sieves (residual water: 10–20 ppm) and destilled under Ar pressure of 1 mbar. As supporting electrolytes, 0.5 M $LiClO_4$ (dried at 300 °C, 1 mbar) or 0.2 M Tetrabutylammoniumhexafluorophosphate ($TBAPF_6$, dried at 170 °C, 1 mbar) have been added to achieve a sufficient conductivity of the electrolyte. For the Fe deposition in addition to the supporting electrolyte, either $FeCl_2$ or $FeCl_3$ (saturation concentration) were dissolved in PC.

Deposition has been done on polycrystalline Pt. A Pt wire dipping in a solution of 0.05 M I_2 and 0.1 M KI in PC served as nonaqueous reference electrode.[18] The experimental handling has been done in an Ar purged glovebag. The residual water content during the deposition was between 100 and 200 ppm.

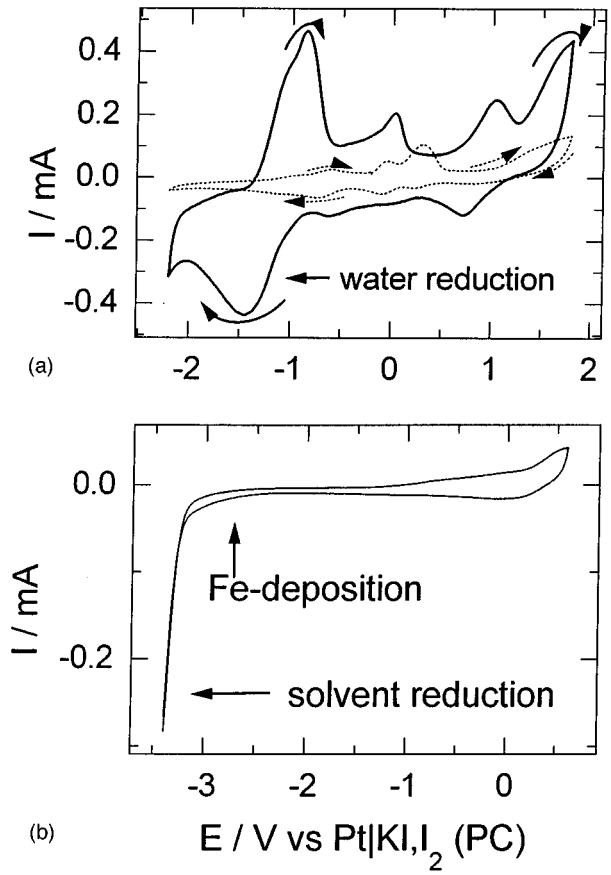

FIG. 4. (a) Background currents using a 0.5 M $LiClO_4$/PC solution (solid curve) or a 0.2 M $TBAPF_6$/PC solution (dotted curve), without the addition of Fe salts. The potential is cycled between -2.2 and $+1.8$ V at 100 mV/s in the direction indicated by the arrows. The peaks in the current–voltage characteristics due to reactions of impurities are much smaller with $TBAPF_6$. (b) Fe deposition on a Pt electrode from a 0.2 M $TBAPF_6$/PC solution saturated with $FeCl_2$ (10 mV/s). The potential sweep range of (a) has been limited to a potential range relevant for the Fe deposition. This results in a decrease of the background current to less than 20 μA. No other features can be observed at potentials higher than the electrolyte decomposition.

In order to deposit Fe from nonaqueous aprotic solutions with a ML charge resolution in the current–voltage characteristics, the background currents must be low as in the case of aqueous solutions (see Fig. 1). A comparison of $LiClO_4$ and $TBAPF_6$ (without the Fe salt present) shows, that the background current is much lower with the organic supporting electrolyte [Fig. 4(a)]. A major reason for this is the participation of the Li^+ ion in different side reactions of the solvent, residual water, and oxygen.[19] The background current as seen in Fig. 4(a) can be further reduced by a limitation of the potential sweep range to below ≈ 0 V avoiding unwanted electrolyte reactions [Fig. 4(b)].

Fe has been deposited from PC with $LiClO_4$ as well as with $TBAPF_6$ [Fig. 4(b)] as supporting electrolyte. Both iron salts, $FeCl_2$ and $FeCl_3$, allow the deposition. The onset of the deposition has been found at potentials around -2.5 V, depending on the electrolyte composition. Thick deposits have been identified as metallic Fe by electron beam induced x-ray emission.

ACKNOWLEDGMENT

We are indebted to H. Menge for the preparation of the Cu crystals.

[1] S. Z. Hua, D. S. Lashmore, L. Salamanca-Riba, W. Schwarzacher, L. J. Swartzendruber, R. D. McMichael, L. H. Bennett, and R. Hart, J. Appl. Phys. **76**, 6519 (1994).
[2] S. K. J. Lenczowski, C. Schönenberger, M. A. M. Gijs, and W. J. M. de Jonge, J. Magn. Magn. Mater. **148**, 455 (1995).
[3] M. Alper, K. Attenborough, R. Hart, S. J. Lane, D. S. Lashmore, C. Younes, and W. Schwarzacher, Appl. Phys. Lett. **63**, 2144 (1993).
[4] B. M. Lairson, J. Perez, and Ch. Baldwin, Appl. Phys. Lett. **64**, 2891 (1994).
[5] S. K. Kim, J. S. Kang, J. I. Jeong, J. H. Hong, Y. M. Koo, H. J. Shin, and Y. P. Lee, J. Appl. Phys. **72**, 4986 (1992).
[6] J.-H. Kim and S.-C. Shin, Jpn. J. Appl. Phys. **35**, 342 (1996).
[7] C.-J. Lin and G. L. Gorman, Appl. Phys. Lett. **61**, 1600 (1992).
[8] C. Wisniewski, I. Denicolo, and I. A. Hümmelgen, J. Electrochem. Soc. **142**, 3889 (1995).
[9] S. Yoshimura, S. Yoshihara, T. Shirakashi, and E. Sato, Electrochim. Acta **39**, 589 (1994).
[10] D. Y. Li and J. A. Szpunar, J. Mater. Sci. **28**, 5554 (1993).
[11] G. Pimenta, V. Schröder, and W. Kautek, Ber. Bunsenges. Phys. Chem. **95**, 1470 (1991).
[12] Y. Jyoko, S. Kashiwabara, and Y. Hayashi, Mater. Trans. JIM **33**, 211 (1992).
[13] W. Schindler and J. Kirschner, Phys. Rev. B **55**, R1989 (1997).
[14] W. Schindler and J. Kirschner, Rev. Sci. Instrum. **67**, 3578 (1996).
[15] A. Rabe, N. Memmel, A. Steltenpohl, and Th. Fauster, Phys. Rev. Lett. **73**, 2728 (1994).
[16] J. Giergiel, J. Kirschner, J. Landgraf, J. Shen, and J. Woltersdorf, Surf. Sci. **310**, 1 (1994).
[17] A. K. Schmid and J. Kirschner, Ultramicroscopy **42–44**, 483 (1992).
[18] J. F. Coetzee and C. W. Gardner, Anal. Chem. **54**, 2530 (1982).
[19] D. Aurbach and A. Zaban, J. Electrochem. Soc. **141**, 1808 (1994).